The Coupled CFD/Free-Wake Method for Numerical Prediction of Rotor BVI Noise

Wang Fei, *Xu Guohua* *, *Hu Zhiyuan*

National Key Laboratory of Science and Technology on Rotorcraft Aeromechanics, College of Aerospace Engineering, Nanjing University of Aeronautics and Astronautics, Nanjing 210016, P. R. China

(Received 25 June 2018; revised 9 August 2018; accepted 26 August 2018)

Abstract: A coupled Navier-Stokes/free-wake method is developed to predict the rotor aerodynamics and wake. The widely-used Farassat 1A formulation is adopted to predict the rotor noise. In the coupled method, the Reynolds-averaged Navier-Stokes (RANS) solver is established to simulate complex aerodynamic phenomena around blade and the tip-wake is captured by a free-wake model without numerical dissipation in the off-body wake zone. To overcome the time-consuming of the coupling strategy in previous studies, a more efficient coupling strategy is presented, by which only the induced velocity on the outer boundary grid need to be calculated. In order to obtain blade control settings, a delta trimming procedure is developed, which is more efficient than traditional trim method in the calculation of Jacobian matrix. Several flight conditions are simulated to demonstrate the validity of the coupled method. Then the rotor noise of operational load survey (OLS) is studied by the developed method as an application and the computational results are shown to be in good agreements with the available experimental data.

Key words: helicopter; rotor; coupled N-S/free-wake method; delta trim method; BVI noise

CLC number: V211.52 **Document code**: A **Article ID**: 1005-1120(2018)05-0800-12

0 Introduction

Helicopter rotor noise, especially the blade-vortex interaction (BVI) noise, has a significant impact on ground observers. The BVI noise occurs in low speed and descending flight conditions, where the generated tip wakes remain within the vicinity of the rotating blades. The close interaction between tip wakes and the blades leads to impulsive fluctuation of blade air-loadings and strong BVI noise[1]. Therefore, an accurate numerical model that is able to capture the rotor wakes and predict the fluctuation of blade air-loadings is necessary for simulation of BVI noise. Meanwhile, the trimming procedure should be incorporated in numerical schemes to match the rotor thrust and eliminate the rotor moments. However, in previous studies, the control inputs are usually obtained from experimental data and the rotor has barely been trimmed by computational fluid dynamics (CFD) method in numerical simulation in most of the previous studies. This is because the complexity and computational time comsumption will have a significant crease dramatically with the traditional trimming method. Therefore, it is also necessary to develop a more efficient rotor trim method for obtaining the accurate blade control settings.

There exist three kinds of approaches in the simulation of rotor aerodynamics and tip wakes, e. g. CFD method[2], potential/wake method[3] and the coupled CFD/wake method[4]. The CFD method is capable of capturing the wakes as part of the solution and has been achieved rapid improvements in past decades. But the application of CFD method is limited due to low computation efficiency and severe numerical dissipation[4]. On the contrary, in free-wake method, the rotor

* Corresponding author, E-mail address: ghxu@nuaa.edu.cn.

How to cite this article: Wang Fei, Xu Guohua, Hu Zhiyuan. The coupled CFD/free-wake method for numerical prediction of rotor BVI noise[J]. Trans. Nanjing Univ. Aero. Astro., 2018, 35(5): 800-811.
http://dx.doi.org/10.16356/j.1005-1120.2018.05.800

wake can be preserved long distance without numerical dissipation. But the free-wake method cannot simulate the viscous effects around blades. The coupled CFD/wake method combines the advantages of CFD method in simulating of compressibility/viscous effects and wake method in rotor wake capturing. In coupled method, the CFD (Euler or Navier-Stokes equation) method is used to calculte the flow-field around the blade and the wake method is employed to capture the tip wake in wake region. It is computationally efficient with a good numerical precision and receives more and more attention. Zhao et al.[5], Berkman et al.[6] developed an N-S/full potential/free-wake coupled method for the simulation of rotor flows, respectively, and the predicted results are in good agreement with the experimental data. However, the complexity of the method is increased by the flowfield transform among the three different computation domains. Afterwards, Sitaraman et al.[7] presented a coupled N-S/free-wake method and also established the field-velocity method for passing the velocity from free-wake to CFD domain. In the field-velocity method, the induced velocities on all the grid points are incorporated via grid movement in CFD solution. Accordingly, the geometric conservation law (GCL) is enforced to satisfy the conservative relations of areas and volumes of the control cells. Accordingly, there is the fault of large calculation quantity for the "field-velocity method". Sugiura et al.[8] studied the coupled Euler/prescribed wake method, but the prescribed wake has low accuracy of calculation.

As pointed out in Ref. [9], inaccurate numerical results may be obtained without incorporating a trimming procedure in aerodynamic model. In previous rotor aerodynamics studies, the traditional trimming procedure[9] is directly incorporated to the numerical schemes. For example, Kim et al.[10] incorporated the trimming procedure to a rotor CFD solver. To match the aerodynamic parameters to the desired levels, 20 revolutions of CFD solver are run with their solver. The researchers developed an efficient trim method[11], in which the time-consuming calculation of Jacobian matrix is conducted by the simple rotor inflow model. This provides an idea on the establishment of efficient trim method in coupled method.

In view of this, a coupled N-S/free-wake method with an efficient trimming procedure is presented for the calculation of BVI aerodynamics in this paper. In this method, the coupling strategy called "outer boundary correction approach" is established. Furthermore, a delta trimming procedure is developed based on the "delta idea", In the procedure, the time-consuming computation of Jacobian matrix is performed by the efficient free-wake method instead of CFD method. And the numerical cases at several flight conditions are calculated to validate the method and illustrate the improvement of the proposed method. Then, combing the coupled CFD/free-wake method with the well-known FW-H equation, a methodology for the prediction of rotor BVI noise is established. The BVI noise of the widely-used operational load survey (OLS) helicopter rotor is calculated by the developed methodology. It is shown that BVI noise energy is mainly radiated to the 120° azimuth and 45° elevation.

1 Rotor Aerodynamic Model

Fig. 1 shows a schematic of the coupled model. In this model, the N-S based CFD method is employed to predict the blade air-loadings and complex aerodynamic phenomena, while a pseudo-implicit predictor-corrector free-wake method[12] is used to capture the rotor tip-wake without dissipation. For coupling algorithm between the two computation domains, an "integrated vorticity approach"[13] and an "outer boundary correction approach" are adopted. The details of the coupled method are described in Fig. 1.

1.1 Coupled method of CFD and free-wake model

1.1.1 N-S based CFD solver

A three dimensional unsteady compressible N-S equation[14] is used as the governing equation of CFD

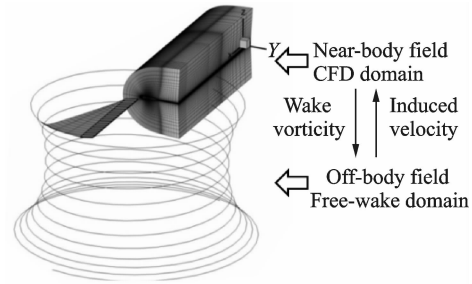

Fig. 1 Schematic of the proposed CFD/free-wake coupled method

$$\frac{\partial}{\partial t}\iiint_V \boldsymbol{W}\mathrm{d}V+\iint_{\partial S}[\boldsymbol{F}(\boldsymbol{W})-\boldsymbol{G}(\boldsymbol{W})]\,\mathrm{d}S=0 \quad (1)$$

where

$$\boldsymbol{W}=\begin{bmatrix}\rho\\ \rho u\\ \rho v\\ \rho w\\ \rho e\end{bmatrix} \quad \boldsymbol{F}=\begin{bmatrix}\rho(\boldsymbol{q}-\boldsymbol{q}_b)\\ \rho u(\boldsymbol{q}-\boldsymbol{q}_b)+p\bar{n}_x\\ \rho v(\boldsymbol{q}-\boldsymbol{q}_b)+p\bar{n}_y\\ \rho w(\boldsymbol{q}-\boldsymbol{q}_b)+p\bar{n}_z\\ \rho H(\boldsymbol{q}-\boldsymbol{q}_b)+p\boldsymbol{q}_b\end{bmatrix}$$

$$\boldsymbol{G}=\begin{bmatrix}0\\ \tau_{xx}\bar{n}_x+\tau_{yx}\bar{n}_y+\tau_{zx}\bar{n}_z\\ \tau_{xy}\bar{n}_x+\tau_{yy}\bar{n}_y+\tau_{zy}\bar{n}_z\\ \tau_{xz}\bar{n}_x+\tau_{yz}\bar{n}_y+\tau_{zz}\bar{n}_z\\ \Phi_x\bar{n}_x+\Phi_y\bar{n}_y+\Phi_z\bar{n}_z\end{bmatrix} \quad (2)$$

In the above equations, $\boldsymbol{W}$ is the vector of conserved variables. $\boldsymbol{F}(\boldsymbol{W})$ and $\boldsymbol{G}(\boldsymbol{W})$ are the convective (inviscid) and the viscous flux vectors, respectively, $\boldsymbol{q}$ and $\boldsymbol{q}_b$ the absolute velocity and the blade moving velocity, respectively. The blade moving velocity includes blade rotation, flapping and pitching motions; p, ρ and e represent pressure, density and energy, respectively. V is the grid cell volume, S the grid surface aream, $\boldsymbol{n}$ the normal vector of grid surface, $\boldsymbol{\Phi}$ the viscous stresses, and $\boldsymbol{\tau}$ the components of the viscous stress tensor.

The inviscid terms are computed with a second-order upwind Roe scheme[15] and the viscous terms are computed by second-order central differencing. For the time integration, a dual-time stepping algorithm is employed with the LU-SGS scheme[16] to simulate the unsteady flow phenomenon at every pseudo-time step. The Spalart-Allmaras turbulence model[17] is applied to the closure RANS equation.

1.1.2 Free-wake model

The rotor wake is composed of near wake and far wake. In the CFD/free-wake coupled method, the near-wake is simulated directly by CFD method. The far-wake comprises only a single tip vortex filament. It evolves from a roll-up of the near-wake detached from the trailing edge of blade after revolving 30°. The motion equation of a vortex filament can be written as[3]

$$\frac{\mathrm{d}\boldsymbol{r}(\psi,\zeta)}{\mathrm{d}t}=\boldsymbol{V}(\boldsymbol{r}(\psi,\zeta)) \quad (3)$$

where $\boldsymbol{r}(\psi,\zeta)$ denotes the positions of control points, ψ the azimuth at which the blade located, ζ the wake age angle, and $\boldsymbol{V}(\boldsymbol{r}(\psi,\zeta))$ the velocity of control points including free-stream and induced velocities from bound vortex as well as the other vortex filaments. The induced velocities are computed by Biot-Savart law with Scully vortex core model[18] with an initial vortex core radius of $0.2C$ (C is the blade chord).

1.1.3 Coupled strategy between two domains

In the coupled method, it is necessary to pass the vorticity from CFD domain to wake domain and feedback the induced velocity from wake domain back to the CFD domain. In the proposed coupled method, the "integrated vorticity approach" is adopted to pass the vorticity from the CFD domain to the free-wake solution. In this method, the radial distribution of sectional lift coefficient is calculated first by integrating the pressure distributions on blade surfaces by CFD. Then the circulation strength of each blade section is calculated using the Kutta-Joukowski theorem[19]

$$\Gamma=\frac{1}{2}cvC_l \quad (4)$$

where C_l is the sectional lift coefficient and v the local flow velocity.

The "outer boundary correction approach" is used to reflect the influence of rotor wake on CFD domain. Different from the traditional "field-velocity approach"[20], in "outer boundary correction approach", the variables of flow field for only the outer grid is calculated by the following equations

$$\boldsymbol{V}=\begin{bmatrix}u\\ v\\ w\end{bmatrix}=\begin{bmatrix}u_\infty+u_i\\ v_\infty+v_i\\ w_\infty+w_i\end{bmatrix} \quad (5)$$

$$\rho = \left(\frac{a^2}{a_\infty^2}\right)^{1/(\gamma-1)} \tag{6}$$

$$e = \rho\left[\frac{a^2}{\gamma(\gamma-1)} + \frac{u^2+v^2+w^2}{2}\right] \tag{7}$$

$$p = (\gamma-1)\rho\left[e - \frac{u^2+v^2+w^2}{2}\right] \tag{8}$$

$$a^2 = a_\infty^2 + \frac{\gamma-1}{2}[V_\infty^2 - (u^2+v^2+w^2)] \tag{9}$$

where $(u_\infty, v_\infty, w_\infty)$, (u_i, v_i, w_i) are the free-stream velocities and wake-induced velocities, respectively. γ is the ratio of specific heat, a the local mach number and ∞ the free stream.

In the coupled method, the induced velocities need to be calculated at every time step. However, the near wake is computed as part of the CFD solution. To avoid the double counting of the near wake, the first 30° of the wake geometry of the free wake are excluded from the induced-velocity calculations.

1.2 Delta trimming procedure

To simulate the rotor aerodynamics accurately, it is necessary to input the precise blade control settings[12]. An efficient trimming procedure is developed in this paper. The trim means that the desired aerodynamics level (including rotor thrust coefficient, rolling moment and pitching moment coefficient) is matched by adjusting the control settings (including collective and cyclic pitch angle) continually.

The rotor thrust and aerodynamic moment coefficients can be expressed as the function of control settings.

$$\begin{aligned} C_T &= C_T(\theta_0, \theta_{1s}, \theta_{1c}) \\ C_{Mx} &= C_{Mx}(\theta_0, \theta_{1s}, \theta_{1c}) \\ C_{My} &= C_{My}(\theta_0, \theta_{1s}, \theta_{1c}) \end{aligned} \tag{10}$$

where C_T, C_{Mx}, C_{My} denote the rotor thrust, the pitching moment and the rolling moment coefficients, respectively. In the motion of rotor, the blade pitch angle can be described using the first harmonic term of the Fourier series, which can be written as

$$\theta(\psi) = \theta_0 + \theta_{1s}\sin(\psi) + \theta_{1c}\cos(\psi) \tag{11}$$

To trim the rotor, an iterative technique is necessary due to the nonlinear relationship between aerodynamic parameters and control settings. The Newton-Raphson iterative method is used to obtain the correction angles in this paper. The steps obtaining the correction angles include:

Firstly, the initial guess of control settings $(\theta_0, \theta_{1s}, \theta_{1c})^0$ is calculated by Eq. (12)

$$\begin{aligned} \lambda &= -\sqrt{\frac{\sqrt{\mu^4 + C_T^2} - \mu^2}{2}} \\ \frac{C_T}{\sigma} &= \frac{a}{4}\left[\frac{2}{3}\theta_0^0 \frac{\left(1 + 9\frac{\mu^2}{4} - \mu^2\right) + \lambda(1-\mu^2)}{1 + 3\frac{\mu^2}{4}}\right] \end{aligned} \tag{12}$$

where θ_0^0 is the estimated collective pitch angle, σ the rotor solid, λ the induced inflow, and a the lifting-line slope. μ and C_T represent the advance ratio and rotor thrust, respectively.

Secondly, under the initial guess the flow solver (coupled method) is run for the initial aerodynamic parameter $(C_T, C_{Mx}, C_{My})^0$.

Thirdly, with the Newton-Raphson iterative method, the correction angle of control settings $\Delta\boldsymbol{X}$ is calculated. The calculation equations are as follows

$$\begin{aligned} \Delta\boldsymbol{X} &= (\Delta\theta_0, \Delta\theta_{1s}, \Delta\theta_{1c})^{\mathrm{T}} = (\boldsymbol{J})^{-1}\Delta\boldsymbol{Y} \\ \Delta\boldsymbol{Y} &= (C_T^{\text{desire}} - C_T, 0 - C_{Mx}, 0 - C_{My})^{\mathrm{T}} \end{aligned} \tag{13}$$

where $\Delta\boldsymbol{X}$ is the correction angle, $(C_T^{\text{desire}}, 0, 0)^{\mathrm{T}}$ the desired level of aerodynamic parameters, $\Delta\boldsymbol{Y}$ the difference value between calculated results and desired level of aerodynamic parameters, and $\boldsymbol{J}$ the Jacobian matrix, which is calculated by the following equation

$$\boldsymbol{J} = \begin{bmatrix} \frac{\partial C_T}{\partial\theta_0} & \frac{\partial C_T}{\partial\theta_{1c}} & \frac{\partial C_T}{\partial\theta_{1s}} \\ \frac{\partial C_{Mx}}{\partial\theta_0} & \frac{\partial C_{Mx}}{\partial\theta_{1c}} & \frac{\partial C_{Mx}}{\partial\theta_{1s}} \\ \frac{\partial C_{My}}{\partial\theta_0} & \frac{\partial C_{My}}{\partial\theta_{1c}} & \frac{\partial C_{My}}{\partial\theta_{1s}} \end{bmatrix} = \begin{bmatrix} \frac{\Delta C_T}{\Delta\theta_0} & \frac{\Delta C_T}{\Delta\theta_{1c}} & \frac{\Delta C_T}{\Delta\theta_{1s}} \\ \frac{\Delta C_{Mx}}{\Delta\theta_0} & \frac{\Delta C_{Mx}}{\Delta\theta_{1c}} & \frac{\Delta C_{Mx}}{\Delta\theta_{1s}} \\ \frac{\Delta C_{My}}{\Delta\theta_0} & \frac{\Delta C_{My}}{\Delta\theta_{1c}} & \frac{\Delta C_{My}}{\Delta\theta_{1s}} \end{bmatrix} \tag{14}$$

In this research, the Jacobian matrix is computed by the efficient free-wake method using a lifting-line technique. But, the aerodynamic parameters cannot be predicted accurately by the

technique. Accordingly, they are corrected with the results from the coupled method. The trimming method is called "the delta trim method". Taking the rotor thrust coefficient as a example, the correction equations is

$$\Delta C_t = C_T^H(\theta_0^n, \theta_{1c}^n, \theta_{1s}^n) - C_T^F(\theta_0^n, \theta_{1c}^n, \theta_{1s}^n)$$
$$C_T(\theta_0^n + \Delta\theta, \theta_{1c}^n, \theta_{1s}^n) = C_T^F(\theta_0^n + \Delta\theta, \theta_{1c}^n, \theta_{1s}^n) + \Delta C_T \quad (15)$$

where C_T^H, C_T^F denote the aerodynamic parameters calculated by coupled method and free-wake model, respectively. ΔC_T represents the difference value between the two aerodynamic models and it is used to correct the results by lifting-line method in the calculation of Jacobian matrix.

1.3 Acoustic prediction method

Using the blade surface pressure calculated by the coupled method, acoustic prediction is conducted by the widely used Ffowcs-Hawkings (FW-H) equation, which is based on the Lighthill's acoustic analogy. The time domain solution of the equation, which is also called F1A formulation[21], is employed in BVI noise prediction

$$p'(\boldsymbol{x},t) = p_t'(\boldsymbol{x},t) + p_l'(\boldsymbol{x},t) \quad (16)$$

where $p_t'(\boldsymbol{x},t)$, $p_l'(\boldsymbol{x},t)$ are the "thickness noise" and the "loading noise", respectively. "Thickness noise" is associated with blade thickness and is caused by the blade motion. "Loading noise" is caused by loading fluctuations on blade surface. The equations for these two terms are as follows[21]

$$p_t'(\boldsymbol{x},t) = \frac{1}{4\pi}\left(\int_{f=0}\left(\frac{\rho_0 \dot{v}_n}{r(1-M_r)^2}\right)_{\text{ret}} \mathrm{d}s + \int_{f=0}\left(\frac{\rho_0 v_n (r\dot{M}_i \hat{r}_i + c_0 M_r - c_0 M^2}{r^2(1-M_r)^3}\right)_{\text{ret}} \mathrm{d}s\right) \quad (17)$$

$$p_l'(\boldsymbol{x},t) = \frac{1}{4\pi}\left(\frac{1}{c_0}\int_{f=0}\left(\frac{\dot{l}_i \hat{r}_i}{r(1-M_r)^2}\right)_{\text{ret}} \mathrm{d}s + \int_{f=0}\left(\frac{l_r - l_i M_i}{r^2(1-M_r)^2}\right)_{\text{ret}} \mathrm{d}s + \frac{1}{c_0}\int_{f=0}\left(\frac{l_r(r\dot{M}_i \hat{r}_i + c_0 M_r - c_0 M^2}{r^2(1-M_r)^3}\right)_{\text{ret}} \mathrm{d}s\right) \quad (18)$$

where $f=0$ means the integration surface is blade surface. Subscript ret indicates the integration is calculated at retarded time. $\dot{M}_i$, $\dot{l}_i$ and $\dot{v}_n$ denote the rate of variation with respect to the source time.

The flowchart of the calculation of rotor aerodynamics and noise by the preposed CFD/free-wake/FW-H method is given in Fig. 2. The solution is conducted as follows: (1) Estimate the control settings and initialize CFD and free-wake solutions. (2) Calculate the bound circulation and to generate the vorticity of tip-wake. (3) Calculate the motion equation of tip wake and to calculate the induced velocity of out grids. (4) Trim the rotor blades until convergence and calculate the blade surface pressures. (5) Calculate rotor noise.

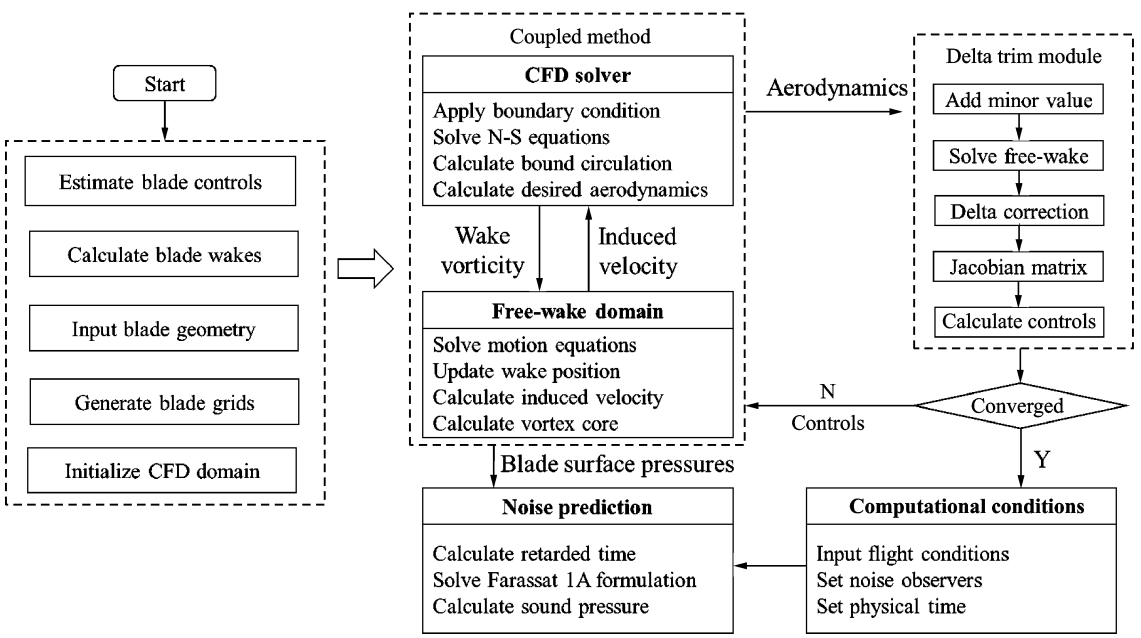

Fig. 2 Flowchart of the proposed CFD/free-wake/FW-H method

It should be pointed out that in CFD domain the time step is set to be 0.25°, while the time step of 1° is used in free-wake solution. The rotor wake geometry between time steps in CFD domain is obtained by the fast Fourier transform interpolation method.

2 Validation of the Coupled Method

2.1 Wake-induced velocity

For coupled method, the induced velocity is important for the accurate prediction of rotor airloadings. The induced velocity for a four-bladed rotor is calculated and compared with the available test data[22], which is measured one chord above the rotor plane. The rotor has a forward shaft tilt of −3°. The blade has a linear twist of −8° from the root to tip and a radius of 0.86 m. The wake-induced velocities are simulated for the case, where thrust coefficient is 0.008 and the advance ratio is 0.15. The comparison of induced velocity between the experimental data and the propsed results is given in Fig. 3. It can be seen from Fig. 3, the proposed results demonstrate agreements with the experimental data. The discrepancies of inflow in central regions may be caused by the presence of fuselage and rotor hub in experiment. The "vortex-induced" upwash effects in the front of the rotor disk is also precisely predicted with the proposed method. Besides, it can be seen that the induced velocities are bigger in the rear of rotor disk from the induced velocities contour. This is because in this flight condition, the wakes are blowed down and backwards to rotor disk.

2.2 The hover case

A numerical case is simulated to discuss the effects of coupling algorithm in coupled method in Fig. 4. The C-T rotor[23] in hover flight is used, where the blade tip mach number is 0.794 and the collective angle is 8°. The rotor has two blades with aspect ratio of 6 and a chord of 0.190 5 m. It can be seen that the results by "outer boundary correction approach" agree better with the experimental data. This is because in "field-velocity ap-

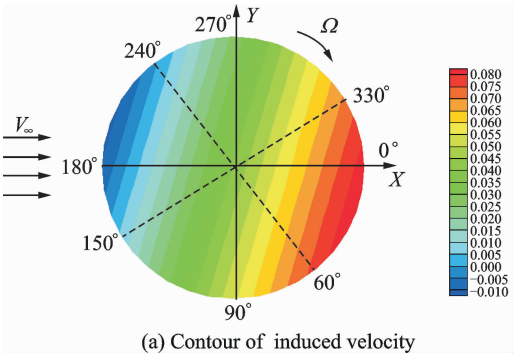

(a) Contour of induced velocity

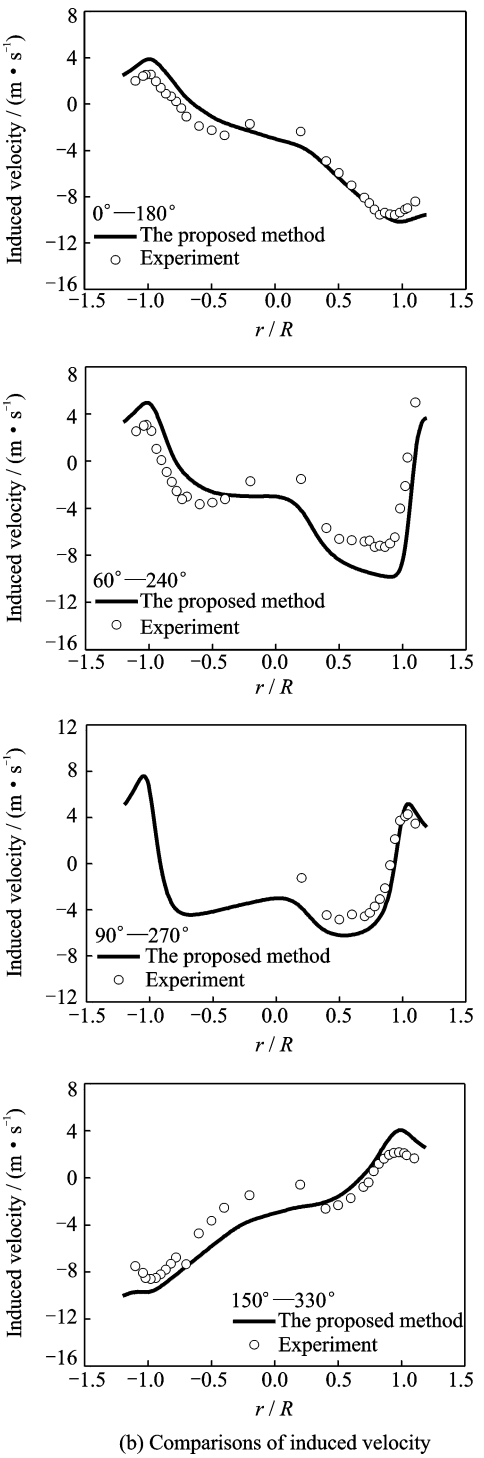

(b) Comparisons of induced velocity

Fig. 3 The calculated induced velocity distribution

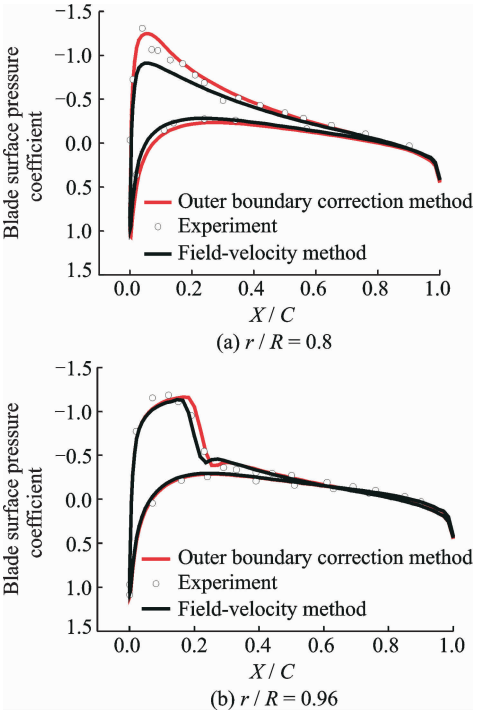

Fig. 4 Comparison of different method for the feedback of wake-induced velocity

proach", the influence of wake-induced velocity on all grid faces in CFD domain is calculated. The result induced velocity on flow field is relatively large[4]. This leads to the blade angle of attack and thus the pressure difference to be small. But, with the increase of rotational speed from the blade inboard regions to the outboard regions, the influence of induced velocity on blade angle of attack diminishes gradually. As a result, the pressure distributions on outboard regions has a better agreement with the experimental data.

By "outer boundary correction approach", a better accordance with experimental data is obtained at all blade span locations.

The blade surface pressure distribution are calculated for the C-T model rotor in hover case by the full CFD (embedded grid CFD) method[24] and the proposed coupled method. Considering the symmetrical characteristics of flow field in hover case, only one blade is modeled. The grid used in full CFD is shown in Fig. 5.

The computation condition is set as follows: thrust coefficient of 0.004 6, hover tip mach number of 0.439. The history of collective angle and thrust coefficient during trimming procedure

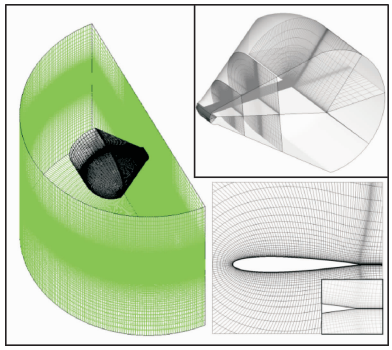

Fig. 5 The generated embedded grid for hover case

is shown in Fig. 6. The trimmed collective angle and thrust coefficient are almost same with the experiment data[23] after 3 trim cycles.

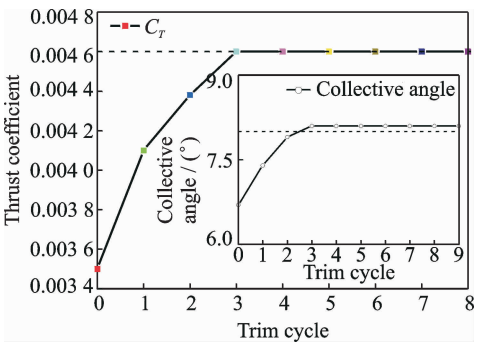

Fig. 6 The history of collective angle and thrust coefficient with trim cycles

The chordwise pressure distribution for several radial stations are simulated by both the coupled method and the full CFD method. The results show good agreements with measurements for both inboard and outboard span locations as seen in Fig. 7.

Under the same condition, the effects of rotor wakes are also analyzed in Fig. 7. The blade pressure are calculated by the proposed coupled method, but in the simulation, the effects of rotor wakes are not coupled. It can be seen that without the rotor wake, the blade surface pressure difference (the dashed dot line in Fig. 7) increases obviously due to the downward induced velocity caused by rotor wake is neglected and the blade angle of attack is enlarged.

The lift coefficient along span is calculated and compared with experiment data in Fig. 8. It can be seen from Fig. 8, although the simulation of aerodynamics is challenging, the calculated re-

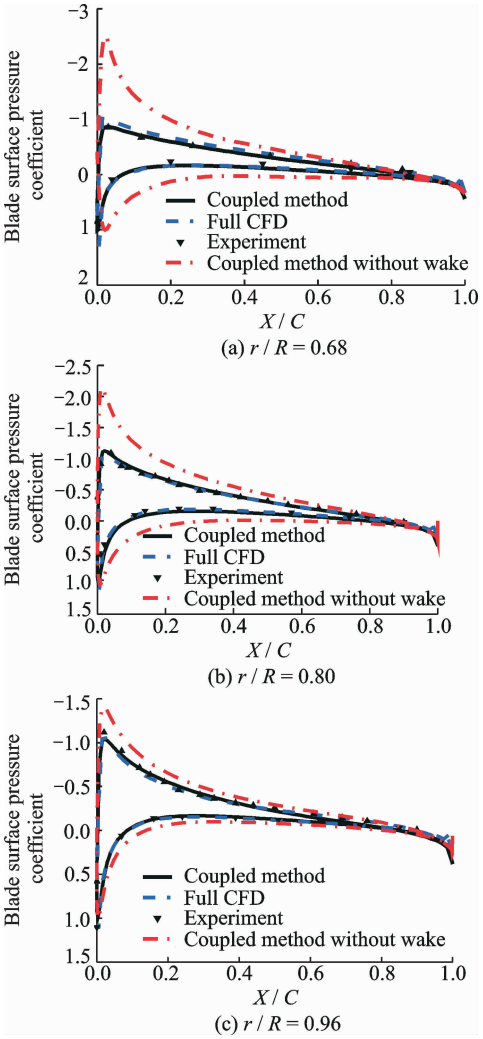

Fig. 7 Chordwise pressure distributions of Caradonna-Tung model rotor

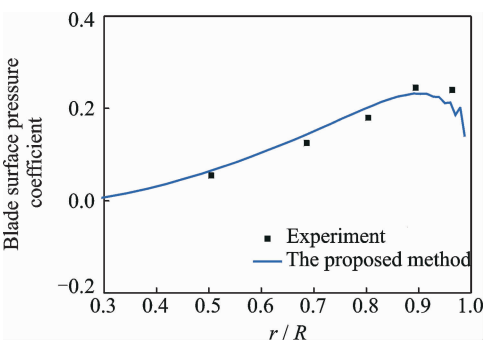

Fig. 8 Sectional lift coefficient distribution along blade span

sults agree with the experimental data well. Only a little discrepancies happen in blade tip region.

Table 1 shows the comparison of computation time between the coupled method and full CFD method under the same number of blade grid. The computations are performed at the PC with Core i7, 3.6 GHz. As shown in Table 1, it takes 20 h to simulate the flow-field for full CFD and 2.5 h for the coupled method. These results indicate that the coupled CFD/free-wake method reduces the computational time dramatically.

Table 1 Comparison of computational time between the two methods

Number of grid	Full CFD method	Coupled CFD/free-wake method
Number of blade grid	239×34×63	239×34×63
Number of background grid	189×148×189	0
Computation time	20 h	2.5 h

2.3 The forward flight case

In this section, the well-known OLS rotor in low-speed descending flight condition is used to validate the capability of coupled method in the calculation of BVI air-loadings, which is very challenging in rotor aerodynamic field. The two-bladed OLS rotor is a 1/7 scale model of AH-1 helicopter main rotor[25]. The blade has an aspect ratio of 9.22 and a linear twist of −8.2°. The control inputs are obtained from the built delta trim method and compared with the experimental data[25] and the results from Ref. [26], as shown in Table 2. Here, θ_0, θ_{1c} and θ_{1s} are the blade collective pitch, longitudinal cyclic pitch and lateral cyclic pitch angles. β_0, β_{1c} and β_{1s} are coning, longitudinal flapping and lateral flapping angles.

Table 2 Control inputs of OLS rotor

Blade motion	θ_0	θ_{1s}	θ_{1c}	β_0	β_{1s}	β_{1c}
Experiment	6.14	−1.39	0.9	0.5	0.0	−1.0
Ref. [26]	6.07	−2.37	1.2	0.5	0.0	−1.0
The proposed	6.51	−2.28	1.5	0.5	0.0	−1.0

To indicate the accuracy and efficiency of the proposed trimming method, the histories of control settings and rotor performance with trim cycles by the traditional trimming method and the proposed delta trimming method are shown in Fig. 9. And the calculation time is summarized in Table 3.

From Fig. 9, it can be seen that the desired aerodynamic values achieve convergence after four to five trim cycles by both methods. Because of the precise coupled model is used to calculate the

Jacobian matrix in the traditional trimming method, it converges slightly faster than the delta trimming model from the aspect of the number of trim cycles. But from Table 3, it can be seen that in traditional trimming model the coupled N-S/free-wake solver runs for 16 revolutions, while the solver runs for only 5 revolutions in delta trimming model. In this case, about 68% computation time is saved.

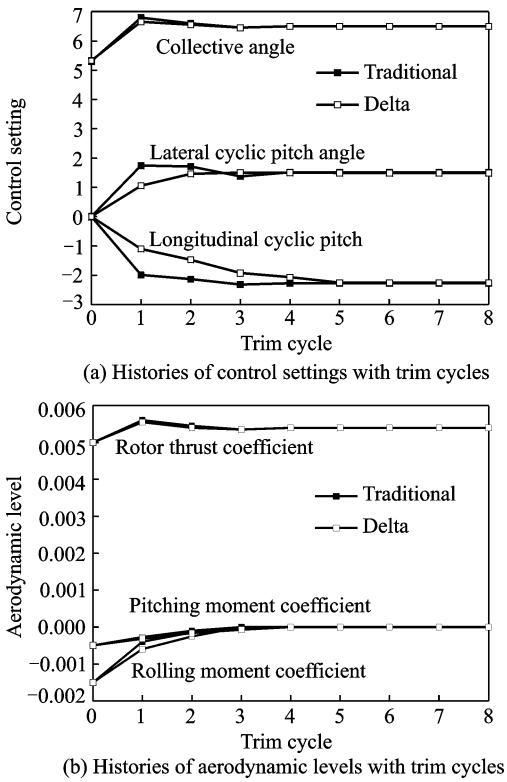

Fig. 9 Histories of control settings and aerodynamic levels with trim cycles

Table 3 Computational time of different trimming methods

Trimming method	Number of trim cycles	Revolutions of coupled solver	Computational time/h
Traditional	4	16	48
Delta	5	5	15.5

Fig. 10 shows the comparison of the predicted blade loads by the proposed method and other three methods (AFDD, DLR, ONERA) from Ref. [27] at 0.91R and 0.95R spanwise locations. It is shown that the predicted value by the proposed method is intermediate compared with other results and has good agreements with them. In addition, the proposed method captures four BVI interactions on the advancing side (#1—#4) and two interactions on the retreating side (#5, #6).

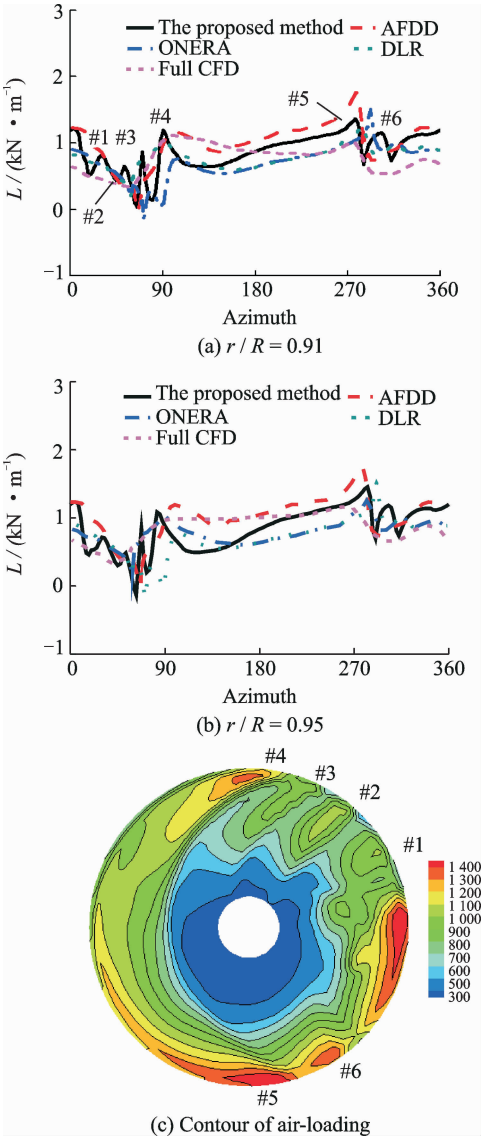

Fig. 10 Comparisons of blade loadings at several spanwise locations and contour of air-loading

These results are in accordance with the theoretical analysis ones from Ref. [27]. While other methods (all belong to wake methods) only capture a single strong interaction. This is because a larger time step is necessary in wake model for the computational convergence[12]. As a result, the interactions between time steps are missed.

To illustrate the importance and contribution of this method, the same case is also simulated by the full CFD method. Although the full CFD method has a minor time step (0.25° is used in this calculation), the numerical dissipation and interpolation errors inherent to the difference schemes employed causes the rotor wake to be modelled with less intensity than that occurs in

physical reality. This is why the blade-vortex interactions are also not captured.

But, it should also be pointed out that the proposed coupled method has a discrepancy on the calculation of blade-vortex interactions occurring at 270° azimuth. This is caused by the integrated vorticity approach, which induces a smaller velocity on the retreating side. In future work, a distributed vorticity approach, which is more complex one, will be included in the solution to improve prediction accuracy.

3 Application of the Coupled Method to Acoustic Analysis

The 10 014 cases in OLS rotor far-field noise tests[25] is applied to predict the BVI noise.

The comparison of noise signals at two observer points is conducted. Both observers are $3.44R$ (R is the rotor radius) away from the rotor hub, 30° below the rotor plane. Laterally, Observers No. 3 and No. 9 are located at $\psi=180°$ and $\psi=210°$, respectively. Locations of the two observers can be identified in Fig. 11.

The comparisons of sound pressure time histories at two different observers among predicted values, experimental data and results from Ref. [27] are shown in Fig. 12. It demonstrates that the proposed method has the capability of capturing two peaks of noise signals and a better agreement with the experimental data. But the method shows a little discrepancy with experimental results locally where rotor noise drops after the second peak.

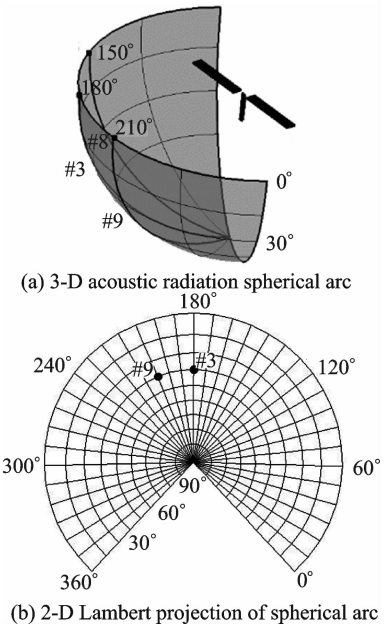

(a) 3-D acoustic radiation spherical arc

(b) 2-D Lambert projection of spherical arc

Fig. 11 Observation locations in radiation sphere

Besides, the comparison of noise signals by the proposed method and the full CFD method is shown in left-hand side of Fig. 12. As shown in Fig. 12, due to the numerical dissipation and interpolation errors in the full CFD method, the rotor wakes are not preserved well and thus the BVI noise amplitudes are not predicted precisely.

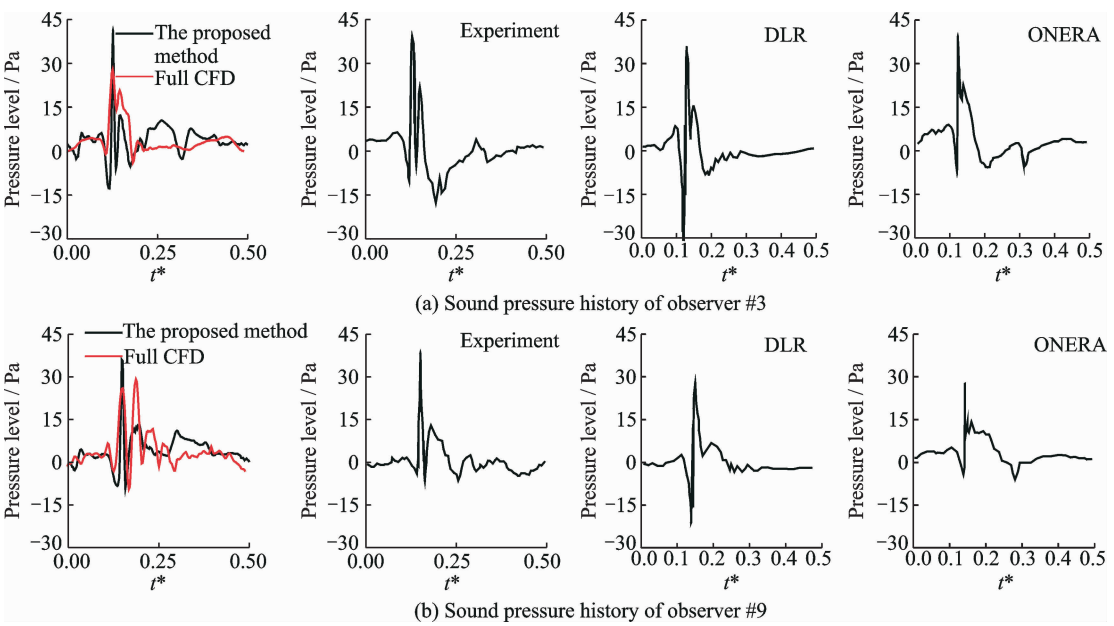

(a) Sound pressure history of observer #3

(b) Sound pressure history of observer #9

Fig. 12 Comparisons of sound pressure time histories at two observer locations

Sound-pressure level (SPL) contours of the acoustic hemisphere is shown in Fig. 13. The acoustic hemisphere, where it has a radius of 3.44 R and the distributed observers on the surface have an interval of 5° in azimuth and elevation direction, is plotted by the Lambert projection method[28]. As shown in Fig. 13, the maximum noise level is observed at the 120° azimuth and −45° elevation, which is the preferred direction of BVI noise.

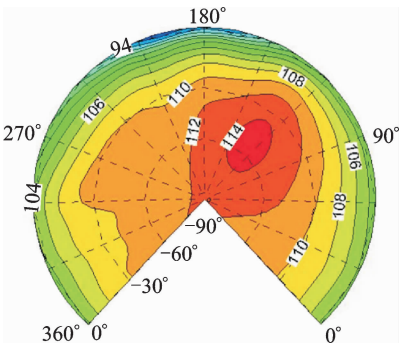

Fig. 13 SPL contours of the OLS rotor

4 Conclusions

A coupled CFD and free-wake method for the prediction of rotor BVI noise is developed with an efficient delta trimming procedure. The method is validated for rotors at hover and forward flight conditions. Based on the FW-H equation, the developed method is used to calculate the rotor BVI noise. The following conclusions can be drawn:

(1) Compared with the field-velocity approach, the outer boundary correction approach is more efficient. The computation time of Jacobin matrix is reduced by the delta trimming procedure due to the efficiency of free-wake model.

(2) From the results regarding the distribution of induced inflow and rotor surface pressure distribution, it can be seen that the proposed coupled method can trim the rotor and predict the BVI aerodynamics accurately.

(3) The fluctuations of air-loadings caused by BVI interaction are fairly well captured with the current coupled method. Compared with wake method and full CFD method, more BVI interactions are captured by the proposed method and the predicted BVI noise by the proposed method agrees with the experimental data.

(4) Rotor BVI noise has strong directivity and it is mainly radiated to 120° azimuth and −45° elevation. This makes the BVI noise more audible to observers on the ground.

References:

[1] BASKARAN B A, BROWN W C. Application of computational fluid dynamics for the dynamic evaluation of rain penetration control[J]. Journal of Molecular Evolution, 1994, 7(3):197-213.

[2] HUANG S, FENG F, YUAN M, et al. Aerodynamic performance and aeroacoustic characteristics of model rotor with anhedral blade tip in hover[J]. Transactions of Nanjing University of Aeronautics & Astronautics, 2018, 35(1):162-169.

[3] Jr CROUSE G L, LEISHMAN J G. A new method for improved rotor free wake convergence[C]//Proceedings of the 31st AIAA Aerospace Sciences Meeting and Exhibit. Reno, Nevada: The American Institude of Aeronautics and Astronautics, 1993:872-881.

[4] INADA Y, YANG C, IWANAGA N, et al. Efficient prediction of helicopter BVI noise under different conditions of wake and blade deformation[J]. Japan Society of Aeronautical Space Sciences Transactions, 2008, 51(173):193-202.

[5] ZHAO Q J, XU G H, ZHAO J G. New hybrid method for predicting the flowfields of helicopter rotors[J]. Journal of Aircraft, 2006, 43(2):372-380.

[6] BERKMAN M E, SANKAR L N, BEREZIN C R, et al. Navier-Stokes/full potential/free-wake method for rotor flows[J]. Journal of Aircraft, 1997, 34(5): 635-640.

[7] SITARAMAN J, BADER J. Evalution of the wake prediction methodologies used in CFD based rotor airload computations[D]. San Francisco, California: American Institute of Aeronautics and Astronautics, 2006.

[8] SUGIURA M, TANABE Y, SUGAWARA H. Development of a hybrid method of CFD and prescribed wake model for helicopter BVI noise prediction[J]. Transactions of the Japan Society for Aeronautical & Space Sciences, 2013, 56(56):343-350.

[9] LORBER P F, STAUTER R C, LANDGREBE A J. A comprehensive hover test of the airloads and airflow of an extensively instrumented model helicopter rotor[C]//Proceedings of the American Helicopter

Society 45th Annual Forum. Boston, MA: [s. n.], 1989.

[10] KIM J W, PARK S H, YU Y H. Euler and Navier-Stokes simulations of helicopter rotor blade in forward flight using an overlapped grid solver: AIAA-2009-4268 [R]. USA: AIAA, 2009.

[11] YANG Z, SANKAR L N, SMITH M J, et al. Recent improvement to a hybrid method for rotors in forward flight[J]. Journal of Aircraft, 2012, 39(5): 804-812.

[12] BAGAI A, LEISHMAN J G. Rotor free-wake modeling using a relaxation technique-including comparisons with experimental data[J]. Journal of the American Helicopter Society, 1995, 40(3): 29-41.

[13] ZHAO J G, HE C J. A hybrid solver with combined CFD and viscous vortex particle method[C]//Proceedings of the 67th Annual Forum of the American Helicopter Society. Virginia Beach, VA: [s. n.], 2011: 393-406.

[14] ZHAO Qijun, ZHU Zheng, YUAN Xin. CFD analyses on effects of blade shape on hover performance of coaxial rigid rotors[J]. Journal of Nanjing University of Aeronautics & Astronautics, 2017, 49(5): 653-661. (in Chinese)

[15] ROE P L. Approximate riemann solvers, parameter vectors, and diffrence schemes[J]. Journal of Computational Physics, 1981, 43(2): 357-372.

[16] LUO H, BAUM J D. A fast, matrix-free implicit method for computing low mach number flws on unstructured grids[D]. San Francisco, California: American Institute of Aeronautics and Astronautics, 1999.

[17] SPALART P R, ALLMARAS S R. An one-equation turbulence model for aerodynamic flows[J]. Recherche Aerospatiale, 1994, 1(1): 5-21.

[18] JOHNSON W. Helicopter theory[M]. Princeton, New Jersey: Princeton University Press, 1980.

[19] SHI Yongjie, ZHAO Qijun, FAN Feng, et al. A new single-blade based hybrid CFD method for hovering and forward-flight rotor computation [J]. Chinese Journal of Aeronautics, 2011, 24(2): 127-135.

[20] KRAEMER E, HERTEL J, WAGNER S. Euler procedure for the calculation of the steady rotor flow with emphasis on wake evolution[C]//Flight Simulation Technologies Conference and Exhibit. Washington, DC: [s. n.], 2013: 132-143.

[21] FARASSAT F. Derivation of formulations 1 and 1A of farassat: NASA Technical Reports Server (NTRS)[R]. Hampton, VA, USA: NASA, 2007.

[22] ELLIOT J W, ALTHOFF S L, SAILEY R H. Inflow measurements made with a laser velocimeter on a helicopter model in forward flight: NASA TM-100542, TM-100543[R]. USA: NASA, 1988.

[23] CARADONNA F X, TUNG C. Experimental and analytical studies of a model helicopter rotor in hover [J]. Vertical, 1981, 5(1): 149-161.

[24] FAN Feng, XU Guohua, SHI Yongjie. Calculations of unsteady aerodynamic interaction between main-rotor and tail-rotor of helicopters based on CFD method[J]. Journal of Aerospace Power, 2014, 29 (11): 2633-2642. (in Chinese)

[25] BOXWELL D A, SCHMITZ F H, SPLETTSTOESSER W R, et al. Helicopter model rotor-blade vortex interaction impulsive noise: Scalability and parametric variations[J]. Erf, 1984, 18(1): 3.

[26] CHUNG K J, HWANG C J, LEE D, et al. Numerical predictions of rotorcraft unsteady air-loading and BVI noise by using a time-marching free-wake and acoustic analogy[C]//31th European Rotorcraft Forum. Firenze, Italy: [s. n.], 2005: 1071-1075.

[27] YU Y H, TUNG C, GALLMAN J, et al. Aerodynamics and acoustics or rotor blade-vortex interaction [J]. AIAA Journal of Aircraft, 1995, 32(5): 970-977.

[28] SNYDER J P. Map projections: A working manual: USGS Paper 1395[R]. Washington, D. C.: U. S. Government Printing Office, 1987.

Mr. **Wang Fei** is a Ph. D. candidate in Aircraft Design at Nanjing University of Aeronautics and Astronautics (NUAA), and his research interests are helicopter CFD and rotor aeroacoustics.

Prof. **Xu Guohua** received his Ph. D. degree in College of Aerospace Engineering at NUAA. His main research interests are helicopter CFD, helicopter aerodynamics and rotor aeroacoustics.

Mr. **Hu Zhiyuan** is a Ph. D. candidate in Aircraft Design at NUAA, and his research interests are helicopter CFD and active control of rotor noise.

(Production Editor: Xu Chengting)